COMMUNICATION

The force of MOFs: the potential of switchable metal–organic frameworks as solvent stimulated actuators†

Pascal Freund,‡[a] Irena Senkovska, [ID][a] Bin Zheng, [ID][bc] Volodymyr Bon, [ID][a]
Beate Krause, [ID][d] Guillaume Maurin [ID][b] and Stefan Kaskel [ID]*[a]

We evaluate experimentally the force exerted by flexible metal–organic frameworks through expansion for a representative model system, namely MIL-53(Al). The results obtained are compared with data collected from intrusion experiments while molecular simulations are performed to shed light on the re-opening of the guest-loaded structure. The critical impact of the transition stimulating medium on the magnitude of the expansion force is demonstrated.

Metal–organic frameworks (MOFs) have been the focus of scientific research for many years due to their diverse properties in the field of surface chemistry and porous materials.[1–3] The development of ever new MOFs with different topologies and chemical features has produced materials promising for a variety of potential applications such as catalysis, gas storage/separation, sensor technology or drug delivery.[4–7] More recently, MOFs have been envisaged for mechanical energy storage[8] and actuators.[9] Switchable coordination polymers, which belong to the third generation of flexible MOFs,[10] undergo stimuli-induced structural transitions. Some of these flexible MOFs exhibit structural transitions at high mechanical pressures and huge changes in their unit cell volumes resulting in remarkable energy storage capacity during 1 cycle of compression/decompression.[11] A prototypical flexible MOF with good chemical stability is MIL-53(M) (MIL = Materials of ínstitute Lavoisier; M = Fe^{3+}, Al^{3+}, Ga^{3+}, In^{3+} or Sc^{3+}), which is formed by corner sharing metal octahedra and terephthalate linkers that create a wine-rack like structure with one dimensional pores.[12] After synthesis and subsequent activation in absence of guest molecules, this materials in its Cr and Al forms are initially present in a large pore or open pore (lp or op) form. Exposure to various fluids or mechanical pressure then leads to a structural transformation to the narrow pore or contracted pore (np or cp) phase, correspondingly, which results in a change of the unit cell volume of about 40% (Fig. S1, ESI†).[13–16] The phase transitions stimulated by mechanical pressure have already been studied for Cr and Al versions of MIL-53 showing promising properties: MIL-53(Cr) as nano-damper[13] and MIL-53(Al) as shock absorber.[16] These investigations were carried out computationally by forcefield/quantum-based molecular simulations[13,16] or thermodynamic models[14,15] and experimentally by combining X-ray diffraction and intrusion of either mercury or oil.[14,16–18] Although these hydrostatic compression/decompression experiments revealed MIL-53 materials as potential energy storage media, they neglected the influence of packing effects, which are expected to play a major role in real applications.[19–22] Moreover, for MIL-53(Al) only the mechanically induced op to cp transformation could be studied, since this structural transition was found to be irreversible and the material remains in its cp form upon decompression.[16]

For the use of MOFs as actuators it is necessary to estimate the force exerted by the MOF upon uptake of guest species. Hence, in the following we present a new strategy for the experimental determination of the expansion force (np to op transition) of compacted powders of switchable MOFs upon adsorption of solvents. It requires no preparation-intensive setups and only short measuring times. The measurements themselves were carried out on a customized measuring system (Fig. 1), which is easy to build.[23] It consists of a standard force measuring bench with a stamp for force transmission, a height measuring device and a cylinder as sample vessel. For the measurement, a defined quantity of MOF powder has to be transferred into the cylinder and compressed to the packing density of interest. The stamp is connected to a motor as well as a force gauge and can move to a specified position with an accuracy of 0.01 mm while simultaneously measuring the pressure applied to the powder to compact it. After compression to a defined packing density, the stamp is moved 0.1 mm

[a] *Inorganic Chemistry I, Technische Universität Dresden, Bergstraße 66, 01062 Dresden, Germany. E-mail: stefan.kaskel@tu-dresden.de*
[b] *ICGM, Univ. Montpellier, CNRS, ENSCM, Montpellier, France*
[c] *School of Materials Science and Engineering, Xi'an University of Science and Technology, Xi'an 710054, P. R. China*
[d] *Leibniz-Institut für Polymerforschung Dresden e.V., Hohe Straße 6, 01069 Dresden, Germany*
† Electronic supplementary information (ESI) available: Experimental details, computational model and method, PXRD patterns, Rietveld plot for MeOH@-MIL-53(Al). See DOI: 10.1039/d0cc02505d
‡ Trevira GmbH, Förster Str. 54, 03172 Guben, Germany.

Fig. 1 Schematic illustration of the developed setup; MOF crystals are simplified as springs and change their volume upon adsorption of solvent causing the specific expansion force to be measured.
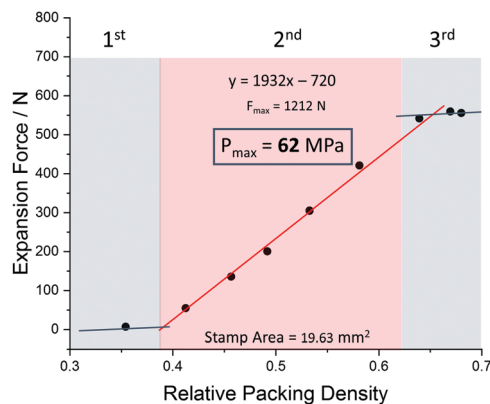
Fig. 2 Expansion force measurements of a compressed powder of MIL-53 (Al) and methanol as solvent with inserted trend line and calculated maximum force for a relative packing density of 1.

above the powder and is fixed at this position, whereby the measured pressure drops to 0.

The adsorptive (solvent or gas) can pass the stamp edge to wet the powder causing the crystals expansion after adsorption in a constant volume. While they push against the stamp, the measured force corresponds to the expansion force exerted by the crystals. The measured expansion forces of the flexible MOF can be plotted against its relative packing densities for a given solvent where each point of the curve corresponds to one measurement of the expansion force of the compressed powder. The packing density of the MOF in the cylinder can be calculated using known parameters such as mass and volume of the compressed powder and the density of the material obtained from the crystal structure. Using the described instrumentation, MIL-53(Al) was studied as model flexible MOF system upon adsorption of liquids such as methanol, ethanol and water. This method allows the comparison of expansion forces for various solvents.

MIL-53(Al) was synthesized and activated as described elsewhere (for details see ESI†). For the measurement, MIL-53 has to be transformed into the np form which can be easily achieved by handling it in air atmosphere, as it was confirmed by X-ray diffraction analysis (Fig. S2, ESI†). Therefore, no pressure or other applied energy is needed for the pre-conditioning of the sample. Upon adsorption of methanol or ethanol, the np to op transition takes place. The crystal structure of MeOH@MIL-53(Al) was refined and it could be shown, that the methanol treatment leads to the expansion of the structure, at which the unit cell volume increases up to *ca.* 55% (Fig. S3 and Table S1, ESI†).

The pre-conditioned MIL-53(Al) samples (np) were transferred into the force-measuring setup (Fig. 1), compacted to defined density and exposed to methanol. The diagram in Fig. 2 shows the results obtained. The measured expansion force profile can be clearly divided into 3 domains: (I) at low packing density, the powder is still very loose, resulting in many larger voids between the crystals. As the crystals expand, they can easily move into these voids, causing only a small force exerted. (II) When the packing density increases, free voids between the crystals are reduced.

Hence the crystals cannot expand into voids further and press stronger on the stamp. In this area, a linear correlation between the packing density and measured expansion force can be observed. (III) At high relative densities, where the empty space fraction approaches the volume expansion upon structural transformation, it ends in a plateau. In this region, the powder cannot be compressed any further to the higher packing densities, without resulting in a certain backpressure to the stamp, even after lifting it for 0.1 mm. The powder shows a spring-like behaviour, resulting in detectable pressures even before the solvent is added.

In order to be able to make a prediction of the theoretical maximum expansion force of a single crystal, the linear range of the measurement can be extrapolated *via* a linear regression to calculate the expansion force for relative packing densities up to 100%. The pressure obtained from such extrapolation for MIL-53(Al) is 62 MPa in the case of methanol, corresponding to the force of 1.2 kN. This value clearly exceeds the pressures measured by intrusion of mercury and oil to induce the op–cp phase transition (13–18 MPa and 33 MPa, respectively).[16,24] From mechanical equations of state published previously for MIL-53(Al)[15] it is also evident, that the external pressure needed to contract the framework is much smaller than the "negative pressure" required for the framework opening.

Flexible force field molecular dynamics (MD) simulations were further performed to unravel the microscopic mechanism at the origin of the re-opening of the structure. Besides the accuracy of the intermolecular force field parameters required to describe the host/guest interactions, these calculations strongly rely on intra-molecular force field parameters to correctly capture the structural behavior of the highly flexible MOFs which is by far more challenging.[8,21,25–28] Therefore, these calculations were achieved on the MIL-53(Cr) framework since our previously-derived flexible force field including intra- and inter-molecular terms for the MIL-53 framework was trained and validated for this Cr-version (corresponding equations and parameters reminded in Table S2, ESI†).[13] The robustness of this flexible force field was recently confirmed by an excellent agreement between the predicted structural behavior of MIL-53(Cr) under the simultaneous application of
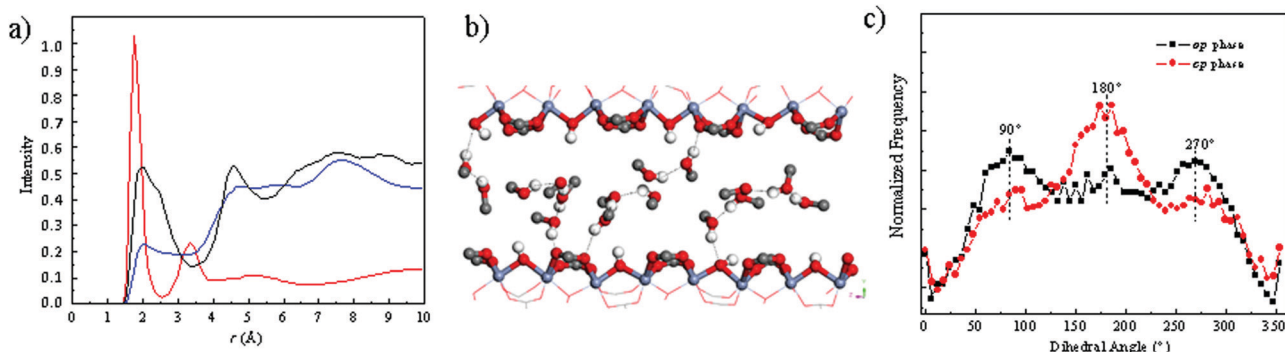
Fig. 3 MD simulations on methanol loaded MIL-53(Cr). (a) Radial distribution functions calculated for the O(methanol)−H(methanol) (red), H(methanol)−O(μ-OH) (black) and H(methanol)−O(carboxylate) (blue) pairs in the np form, (b) illustration of the methanol arrangement in the np form with a view along the channel and (c) (C−O⋯O−C) dihedral angle formed between adjacent methanol molecules in the np and op forms.

mechanical pressure and guest adsorption and that of its MIL-53(Al) analogue evidenced experimentally.[29]

This force field for MIL-53(Cr) was further combined with the well-trained generic TraPPE-UA[30] force field for methanol to describe the behavior of the methanol-loaded MIL-53(Cr) system. Once adsorbed in the np form, methanol molecules establish hydrogen bonds between themselves with characteristic O(methanol)–H(methanol) distances of 1.80 Å as evidenced by the radial distribution functions (RDFs) calculated for the corresponding atoms pair (Fig. 3a). In addition methanol interacts strongly with the MOF pore wall *via* its hydrogen atoms with either the oxygen atoms of the μ-OH groups or the oxygen atoms of the carboxylate groups with characteristic H(methanol)–O(μ-OH) distances of 2.00 Å and H(methanol)–O(carboxylate) distances of 2.03 Å (see corresponding RDFs in Fig. 3a). Such a geometric arrangement of methanol is illustrated in Fig. 3b. We further evidenced that the np–op transition of the framework resulting from the rotation of the phenyl ring about the O–O axis of the carboxylate is accompanied by a significant change of the orientation of the methanol molecules with respect to each other. Indeed Fig. 3c shows that the molecules initially in the np form mostly coplanar with an associated preferential (C–O⋯O–C) dihedral angle of 180° are significantly tilted from each other once the structure switches to the op form, the contributions of the corresponding dihedral angle being at 90° and 270°. The methanol loaded MIL-53(Cr) contracts only under high external pressure applied (90 MPa), this structural switching being reversible upon mechanical release with a small hysteresis of 5 MPa (Fig. S5, ESI†). Hence, 85 MPa may represent the maximum force/pressure the framework can sustain. For MIL-53(Al) this pressures is expected to be lower, and in our experimental force measurements, the fluid pressure is atmospheric. Hence, the force of MOF obtained in our experiment (65 MPa) is reasonable.

We further experimentally explored the influence of the nature of the solvent on the magnitude of the expansion force and the associated pressure. Fig. 4 shows that the use of ethanol leads to a pressure of 48 MPa (force of 942 N) which is lower than the value observed for methanol. The adsorption enthalpy measured by microcalorimetry for ethanol (about −50 kJ mol^{-1}) in the op

form of MIL-53(Cr) is slightly higher than the value obtained for methanol (about −45 kJ mol^{-1}).[31] These experimental values are well captured by our GCMC simulations data (see ESI†) which predict an adsorption enthalpy at low coverage of −50.9 kJ mol^{-1} and −46.1 kJ mol^{-1} for ethanol and methanol respectively. However, the amount adsorbed in saturation is found both experimentally[31] and theoretically (ESI†) to be higher for methanol (12 molecules per u.c. for both experiments and simulations) than that for ethanol (experiment: 8 molecules per u. c. and simulation: 7 molecules per u.c.), hence the total enthalpy ($n \cdot \Delta H_{ads}$) per unit cell is higher for methanol, than for ethanol, a possible rational explanation for the smaller force measured for ethanol.

Finally, the use of water as solvent leads, as expected, to no measurable force from the powder (Fig. S4, ESI†), since the strong interactions between the water and the μ-OH group in tandem with the highly oriented hydrogen bonded network formed between the water molecules, previously reported for the hydrated np form,[32] prevent the re-opening of the structure.

In summary, a new method for measuring the solvent stimulated expansion force of switchable metal–organic frameworks was presented using MIL-53(Al) as model system. Expansion forces can be determined in relatively short measuring times

Fig. 4 Expansion force measurements of a compressed powder of MIL-53(Al) and ethanol as solvent with inserted trend line and calculated maximum force for a relative packing density of 1.

with little preparative effort. The sample is measured as compressed powder, which means that packing effects are directly reflected in the data. MIL-53 (Al) shows three areas in the progression of the pattern which are directly dependent on the packing density. In the second, linear range of the measurement, the profile of the curve can be extrapolated by means of a trend line, which allows data to be calculated for the maximum actuation forces. The pressure gained from the opening step was found to be higher than that needed to compress the empty framework and to be specific for the stimulating fluid. All in all, this newly developed experimental set-up is well suited to estimate the actuating force of switchable MOFs for a variety of fluids. The force of MOFs significantly exceeds the (ambient) pressure of the stimulating fluid rendering switchable MOFs as promising solids for actuation devices in microfluidics or macroscopic systems. Enhancing the force of MOFs further may be achievable through: (i) enhanced fluid–pore wall interactions, (ii) reduced pore size of the op-form (implying reduced adsorbate compressibility), and (iii) idealized packings through particle size engineering. Regarding framework architectures a deeper understanding of mechanoresponse may be achievable by AFM techniques probing single crystals. The latter might also give important insights into the anisotropy exerted MOF forces. Beyond actuation, the new measurement technique presented here provides quantitative characteristics important for using switchable MOFs in real world separation applications in which the adsorbent column is several meters high implying severe mechanical forces acting on the adsorbent lower layers critically affecting their responsiveness.

Conflicts of interest

There are no conflicts to declare.

Notes and references

1 H. Furukawa, K. E. Cordova, M. O'Keeffe and O. M. Yaghi, *Science*, 2013, **341**, 1230444.
2 S. Kitagawa, *Chem. Soc. Rev.*, 2014, **43**, 5415–5418.
3 I. M. Hönicke, I. Senkovska, V. Bon, I. A. Baburin, N. Bönisch, S. Raschke, J. D. Evans and S. Kaskel, *Angew. Chem., Int. Ed.*, 2018, **57**, 13780–13783.
4 C. J. Doonan and C. J. Sumby, *CrystEngComm*, 2017, **19**, 4044–4048.
5 P. Freund, I. Senkovska and S. Kaskel, *ACS Appl. Mater. Interfaces*, 2017, **9**, 43782–43789.
6 M. X. Wu and Y. W. Yang, *Adv. Mater.*, 2017, **29**, 1606134.
7 G. Maurin, C. Serre, A. Cooper and G. Férey, *Chem. Soc. Rev.*, 2017, **46**, 3104–3107.
8 P. G. Yot, L. Vanduyfhuys, E. Alvarez, J. Rodriguez, J.-P. Itié, P. Fabry, N. Guillou, T. Devic, I. Beurroies and P. L. Llewellyn, *Chem. Sci.*, 2016, **7**, 446–450.
9 J. Troyano, A. Carné-Sánchez, J. Pérez-Carvajal, L. León-Reina, I. Imaz, A. Cabeza and D. Maspoch, *Angew. Chem., Int. Ed.*, 2018, **57**, 15420–15424.
10 S. Horike, S. Shimomura and S. Kitagawa, *Nat. Chem.*, 2009, **1**, 695.
11 P. Theato, B. S. Sumerlin, R. K. O'Reilly and T. H. Epps III, *Chem. Soc. Rev.*, 2013, **42**, 7055–7056.
12 C. Serre, F. Millange, C. Thouvenot, M. Nogues, G. Marsolier, D. Louër and G. Férey, *J. Am. Chem. Soc.*, 2002, **124**, 13519–13526.
13 A. Ghoufi, A. Subercaze, Q. Ma, P. G. Yot, Y. Ke, I. Puente-Orench, T. Devic, V. Guillerm, C. Zhong and C. Serre, *J. Phys. Chem. C*, 2012, **116**, 13289–13295.
14 A. V. Neimark, F.-X. Coudert, C. Triguero, A. Boutin, A. H. Fuchs, I. Beurroies and R. Denoyel, *Langmuir*, 2011, **27**, 4734–4741.
15 L. Vanduyfhuys, S. Rogge, J. Wieme, S. Vandenbrande, G. Maurin, M. Waroquier and V. Speybroeck, *Nat. Commun.*, 2018, **9**, 204.
16 P. G. Yot, Z. Boudene, J. Macia, D. Granier, L. Vanduyfhuys, T. Verstraelen, V. Van Speybroeck, T. Devic, C. Serre, G. Férey, N. Stock and G. Maurin, *Chem. Commun.*, 2014, **50**, 9462–9464.
17 P. Serra-Crespo, A. Dikhtiarenko, E. Stavitski, J. Juan-Alcañiz, F. Kapteijn, F.-X. Coudert and J. Gascon, *CrystEngComm*, 2015, **17**, 276–280.
18 I. Beurroies, M. Boulhout, P. L. Llewellyn, B. Kuchta, G. Férey, C. Serre and R. Denoyel, *Angew. Chem.*, 2010, **122**, 7688–7691.
19 C.-h. Liu, S. R. Nagel, D. Schecter, S. Coppersmith, S. Majumdar, O. Narayan and T. Witten, *Science*, 1995, **269**, 513–515.
20 M. Doxastakis, Y.-L. Chen, O. Guzman and J. J. de Pablo, *J. Chem. Phys.*, 2004, **120**, 9335–9342.
21 D. L. Blair, N. W. Mueggenburg, A. H. Marshall, H. M. Jaeger and S. R. Nagel, *Phys. Rev. E: Stat., Nonlinear, Soft Matter Phys.*, 2001, **63**, 041304.
22 W. C. Duncan-Hewitt and G. C. Weatherly, *J. Pharm. Sci.*, 1990, **79**, 147–152.
23 B. Krause, R. Boldt, L. Häußler and P. Pötschke, *Compos. Sci. Technol.*, 2015, **114**, 119–125.
24 J. Rodriguez, I. Beurroies, T. Loiseau, R. Denoyel and P. L. Llewellyn, *Angew. Chem., Int. Ed.*, 2015, **54**, 4626–4630.
25 J. Heinen and D. Dubbeldam, *WIREs Comput. Mol. Sci.*, 2018, **8**, e1363.
26 L. Vanduyfhuys, S. Vandenbrande, T. Verstraelen, R. Schmid, M. Waroquier and V. Van Speybroeck, *J. Comput. Chem.*, 2015, **36**, 1015–1027.
27 M. Tafipolsky and R. Schmid, *J. Phys. Chem. B*, 2009, **113**, 1341–1352.
28 A. R. Kulkarni and D. S. Sholl, *Langmuir*, 2015, **31**, 8453–8468.
29 N. Chanut, A. Ghoufi, M.-V. Coulet, S. Bourrelly, B. Kuchta, G. Maurin and P. L. Llewellyn, *Nat. Commun.*, 2020, **11**, 1216.
30 B. Chen, J. J. Potoff and J. I. Siepmann, *J. Phys. Chem. B*, 2001, **105**, 3093–3104.
31 S. Bourrelly, B. Moulin, A. Rivera, G. Maurin, S. Devautour-Vinot, C. Serre, T. Devic, P. Horcajada, A. Vimont, G. Clet, M. Daturi, J.-C. Lavalley, S. Loera-Serna, R. Denoyel, P. L. Llewellyn and G. Férey, *J. Am. Chem. Soc.*, 2010, **132**, 9488–9498.
32 F. Salles, S. Bourrelly, H. Jobic, T. Devic, V. Guillerm, P. Llewellyn, C. Serre, G. Ferey and G. Maurin, *J. Phys. Chem. C*, 2011, **115**, 10764–10776.